International Journal of Modern Manufacturing Technologies
ISSN 2067–3604, Vol. XI, No. 2 / 2019

ACHIEVING OPTIMAL PARAMETRIC COMBINATION FOR AISI 52100 STEEL HARD TURNING WITH MULTIPLE PERFORMANCE CHARACTERISTICS USING INTEGRATED RSM AND GRA-PCA

Umamaheswarrao Ponugoti [1,2], Ranga Raju Dantuluri [3], Naga Sai Suman Koka[4], Ravi Sankar Bhuvanagiri[5]

[1]Research Scholar, Department of Mechanical Engineering, Andhra University College of Engineering, Visakhapatnam, A.P India PIN-530003
[2]Department of Mechanical Engineering, Bapatla Engineering College, Bapatla, A.P. India PIN-522102
[3]Department of Mechanical Engineering, Srinivasa Institute of Engineering & Technology, Amalapuram, A.P India PIN-533216
[4]Department of Mechanical Engineering, Andhra University College of Engineering, Visakhapatnam, A.P India PIN-530003
[5]Department of Mechanical Engineering, Bapatla Engineering College, Bapatla, A.P. India PIN-522102

Corresponding author: Umamaheswarrao P, maheshponugoti@gmail.com

Abstract: Hard turning evolved to be an efficient alternative offering close proximity to the design dimensions compared to the existing end manufacturing process i.e. grinding. However, setting of optimal machining parameters in hard turning is essential for achieving the high performance. Hence, the present work targeted to perform investigative analysis on the AISI 52100 steel hard turning using Polycrystalline cubic boron nitride (PCBN) tools for optimum machining force, surface roughness and workpiece surface temperature (WST). Experiments are planned and conducted as per Central Composite Design (CCD) of Response Surface Methodology (RSM) by varying the input parameters cutting speed, feed, depth of cut, nose radius and negative rake angle. The objective of the current work demands a scientific approach, hence a sound and proven technique GRA coupled PCA methodology is adopted, multi objective optimization index GRG is computed. The obtained values of GRG are correlated to the input machining parameters by non-linear regression model of second order based on RSM. The agreement of developed model is justified with ANOVA. Investigations on the parametric influence over multi objective index are conferred with the aid of main effects plot and response surface plots generated using the model. From the investigations it is noticed that speed is the major factor affecting the responses followed by negative rake angle, feed, depth of cut and nose radius. The optimum cutting parameters obtained are cutting speed 1000 rpm, feed 0.02 mm/rev, depth of cut 0.4 mm, nose radius 1 mm and negative rake angle 5°. Confirmation test proved the efficacy of adopted methodology and results obtained.

Key words: Hard turning; AISI 52100 steel; Machining force; Surface roughness; Workpiece surface temperature.

1. INTRODUCTION

Manufacturing industry was constantly striving for optimization of the production cost and time in order to maintain competitiveness. The finishing process which effect productivity would be critical in ensuring the quality of the product, usually grinding and polishing operations are rendered for this purpose. However, the existing end processes were reinstated for harder materials by the turning termed as hard turning [1-3]. Hard machining characterizes enhanced material removal rate, more flexibility, less setup time and reduction in machining time, resulting 30% off in machining cost in contrast to grinding [4]. Selection of the most appropriate machining settings was essential for improving cutting efficiency.

Qinghua Li et al. [5] reported that cutting, radial and axial forces were influenced by depth of cut and spindle speed when hard turning of GCr15 steel using PCBN tool. Umamaheswarrao et al. [6] demonstrated that negative rake angle is the most noteworthy factor affecting the responses followed by feed, speed, depth of cut, and nose radius while optimizing process parameters in AISI 52100 steel hard turning. Avinash et al. [7] carried out multi response optimization of machining force and surface roughness in hard turning of AISI 52100 steel using Hybrid GRA-PCA. Results demonstrated that responses were majorly influenced by speed followed by nose radius, feed, and depth of cut.

Amlana Panda et al. [8] concluded that surface roughness was considerably affected by feed and depth of cut during parametric optimization in hard turning of AISI 52100 steel. Dong Min Kim et al. [9] optimized cutting conditions while hard turning of bearing steel using response surface methodology. The results concluded that surface roughness was strongly dependent on cutting speed.

Umamaheswarrao et al. [10] optimized process parameters while hard turning of AISI 52100 steel

using hybrids GRA-PCA. Results established that responses were extensively affected by nose radius subsequently feed, depth of cut and speed.

Depth of cut influenced cutting forces greatly compared to feed rate and cutting speed [11, 12]. Investigations on AISI 52100 steel hard turning with CBN tools reported that feed rate and cutting speed strongly influenced surface roughness [11-14]. Earlier studies revealed that nose radius was the most controlling parameter [15, 16]. In hard turning the surface finish was subjective to workpiece surface temperature (WST) significantly and higher the WST better the surface roughness [17-20]. The sound technique GRA integrated with PCA for multi objective optimization of parameters was performed by Ravi Sankar and Umamaheswarrao [21], Pradhan et al. [22], Vijian and Seshagiri Rao [23], Shailesh Dewangan et al. [24], Umamaheswarrao et al. [25] Campos et al. [26], Eskandari et al. [27] and gained wider success.

The past studies made a large amount of interest to study the outcome of machining conditions on the responses. Scanty literature was available on the influence of tool geometry parameters on the responses and the much interest was focused on nose radius only.

Most of the studies focused on the forces developed and surface roughness during hard turning. However, the WST reported to be the sensible and controlling factor for turning performance. Hence, the present study was aimed to conduct hard turning of AISI 52100 steel using PCBN tools with cutting speed, feed rate and depth of cut as cutting parameters, nose radius and negative rake angle as tool geometry parameters. Machining force, Surface roughness, and WST were considered as responses. Further, multi-objective optimization was performed deploying GRA coupled with PCA for determining optimum cutting conditions.

2. EXPERIMENTAL DETAILS

Turn master-35 type lathe was used and experiments were conducted through variable speed and feed drive in dry condition. Experimental setup was given away in Figure 1. AISI 52100 steel round bar with a hardness of 57HRC, 500mm length and 48mm diameter deployed for the experiment. Machining length and diameter of workpiece was fixed at 30mm and 48mm respectively for every experimental run. PCBN inserts were used with diverse negative rake angles (-5, -15, -25, -35 and -45) and through different nose radii such as r=(0.4, 0.6, 0.8, 1, 1.2)mm. The inserts were mounted in PSBNR2525M12 tool holder. Geometry of the tool-in-holder is specified by the ensuing angles: χr=+75°, λ=−6°, γ=−6°, and α=+6°

Five parameters were varied at five levels throughout experimentation and their effect on responses like machining forces, surface roughness (Ra), and WST were examined.

The Kistler three-component dynamometer model 9257B is used to measure cutting forces. The surface roughness (Ra) of the turned samples was measured with Mitutoyo make Surface roughness tester (SJ-210). WST was measured using an infrared thermometer manufactured by AMPROBE (Range: -50°C to 1550°C, Model: IR 750). Experimental matrix along with obtained results is exposed in Table 1.

Fig. 1. Experimental setup

3. METHODOLOGY ADOPTED

3.1 Hybrid GRA-PCA

Optimum input parameters setting is determined by deploying GRA for enhanced machining performance [28, 29]. The weight contributions of the parameters are calculated through PCA and then multiplied with GRC to obtain GRG [30, 31]. To obtain optimum parametric combinations hybrid GRA PCA is employed. If the performance characteristic is Higher-the-better the following equation (1) is used for normalization:

$$x_i^*(k) = \frac{x_i^0(k) - \min x_i^0(k)}{\max x_i^0(k) - \min x_i^0(k)} \quad (1)$$

If the performance characteristic is smaller-the-better the following equation (2) is used for normalization:

$$x_i^*(k) = \frac{\max x_i^0(k) - x_i^0(k)}{\max x_i^0(k) - \min x_i^0(k)} \quad (2)$$

$x_i^0(k)$ is the measurement of the quality characteristic, $\max x_i^0(k)$ is the largest value of $x_i^0(k)$, $\min x_i^0(k)$ is the smallest value of $x_i^0(k)$

The deviational sequence can be calculated using the equation (3):

$$x_i^*(k) = 1 - \frac{\left| x_i^0(k) - x^0 \right|}{\max x_i^0(k) - x^0} \quad (3)$$

Table 1. Experimental matrix with results

Exp. No	Speed (rpm)	Feed (mm/rev)	Depth of cut (mm)	Nose radius (mm)	Negative rake angle (°)	Machining force (N)	Surface Roughness (Ra) (µm)	Workpiece surface temperature (°C)
1	400	0.04	0.5	0.6	35	404.735	0.525	57.43
2	800	0.04	0.5	0.6	15	233.475	0.465	74.4
3	400	0.08	0.5	0.6	15	322.117	0.453	65.19
4	800	0.08	0.5	0.6	35	473.03	0.545	77.68
5	400	0.04	0.7	0.6	15	317.493	0.552	71.96
6	800	0.04	0.7	0.6	35	376.384	0.507	82.88
7	400	0.08	0.7	0.6	35	583.032	0.539	70.27
8	800	0.08	0.7	0.6	15	380.407	0.471	65.48
9	400	0.04	0.5	1	15	273.585	0.485	66.3
10	800	0.04	0.5	1	35	425.463	0.401	66.3
11	400	0.08	0.5	1	35	561.163	0.507	84.38
12	800	0.08	0.5	1	15	350.276	0.502	80.11
13	400	0.04	0.7	1	35	443.782	0.508	67.07
14	800	0.04	0.7	1	15	323.621	0.408	80.3
15	400	0.08	0.7	1	15	411.791	0.604	68.76
16	800	0.08	0.7	1	35	523.367	0.498	76.5
17	200	0.06	0.6	0.8	25	430.828	0.559	66.61
18	1000	0.06	0.6	0.8	25	355.441	0.456	82.73
19	600	0.02	0.6	0.8	25	309.595	0.468	70.85
20	600	0.1	0.6	0.8	25	534.481	0.53	74.88
21	600	0.06	0.4	0.8	25	344.431	0.45	71.39
22	600	0.06	0.8	0.8	25	449.219	0.48	74.2
23	600	0.06	0.6	0.4	25	359.396	0.514	67.18
24	600	0.06	0.6	1.2	25	446.225	0.485	76.05
25	600	0.06	0.6	0.8	5	279.954	0.484	70.32
26	600	0.06	0.6	0.8	45	601.276	0.509	73.68
27	600	0.06	0.6	0.8	25	358.525	0.507	68.6
28	600	0.06	0.6	0.8	25	370.743	0.518	74.94
29	600	0.06	0.6	0.8	25	378.525	0.52	71.41
30	600	0.06	0.6	0.8	25	403.976	0.512	66.36
31	600	0.06	0.6	0.8	25	380.24	0.488	76
32	600	0.06	0.6	0.8	25	370.65	0.522	69

Grey relational coefficient, $\xi(k)$ and can be calculated as in equation (4):

$$\xi(k)=\frac{\Delta_{\min}+\xi\Delta_{\max}}{\Delta_{0i}(k)+\xi\Delta_{\max}} \quad (4)$$

Absolute difference between $x_i^0(k)$ and $x_i^*(k)$ is called the deviation sequence ($\Delta_{0i}(k)$).The covariance matrix S is formulated with grey relational coefficients as in equation (5):

$$S=\begin{matrix} x_{1,1} & x_{1,2} & .... & x_{1,n} \\ x_{2,1} & x_{2,2} & .... & x_{2,n} \\ ... & ... & ... & ... \\ x_{m,1} & x_{m,2} & ... & x_{m,n} \end{matrix} \quad (5)$$

Where m is a number of experiments, n is a number of quality characteristics, and x is a grey relational coefficient of each quality characteristic.

The correlational coefficient array can be evaluate as

$$R_{jl}=\left(\frac{Cov\left(X_i(j),X_i(l)\right)}{\sigma_{x_i(j)}\times\sigma_{x_i(l)}}\right) \quad \text{j= 1,2..,n l=1,2,3..,n} \quad (6)$$

where Cov($x_i(j)$, $x_i(l)$): the covariance of sequences $x_i(j)$ and $x_i(l)$.
From the correlation coefficient array the eigenvector and eigen values are calculated with equation (7):

$$\left(R-\lambda_k I_m\right)V_{ik}=0 \tag{7}$$

Where λ_k is eigen values $\sum_{k=1}^{n}(\lambda_k)=n$, k= 1,2……n;

$V_{ik}=\left[a_{k,1},\quad a_{k,2}.....\quad a_{k,m}\right]^T$;the eigen vectors correspond to the eigen values, λ_k. Experimental response quality decides weighting value ω_k for each parameter is calculated via PCA. The GRG expressed as in equation (8):

$$x_i=\frac{1}{n}\sum_{k=1}^{n}\omega_k\xi_i(k) \tag{8}$$

Table 2. Normalised values for Machining force, Surface roughness and WST

Exp. No	Machining force	Surface roughness	WST
1	0.534367	0.3891625	0
2	1	0.6847290	0.6296846
3	0.7589946	0.7438423	0.2879406
4	0.3486831	0.2906403	0.7513914
5	0.7715666	0.2561576	0.5391465
6	0.6114502	0.4778325	0.9443413
7	0.0496029	0.3201970	0.4764378
8	0.6005122	0.6551724	0.2987012
9	0.8909464	0.5862068	0.3291280
10	0.4780112	1	0.3291280
11	0.1090616	0.4778325	1
12	0.6824342	0.5024630	0.8415584
13	0.4282043	0.4729064	0.3576994
14	0.7549055	0.9655172	0.8486085
15	0.5151834	0	0.4204081
16	0.2118237	0.5221674	0.7076066
17	0.4634245	0.2216748	0.3406307
18	0.6683913	0.7290640	0.9387755
19	0.7930402	0.6699507	0.4979591
20	0.1816063	0.3645320	0.6474953
21	0.6983259	0.7586206	0.5179962
22	0.4134219	0.6108374	0.6222634
23	0.6576382	0.4433497	0.3617810
24	0.4215622	0.5862068	0.6909090
25	0.8736300	0.5911330	0.4782931
26	0	0.4679802	0.6029684
27	0.6600063	0.4778325	0.4144712
28	0.6267873	0.4236453	0.6497217
29	0.6056291	0.4137931	0.5187384
30	0.5364313	0.4532019	0.3313543
31	0.6009662	0.5714285	0.6890538
32	0.6270401	0.4039408	0.4293135

Table 3. Deviation sequences for Machining force, Surface roughness and WST

Exp. No	Machining force	Surface roughness	WST
1	0.465632	0.610837	1
2	0	0.315270	0.370315
3	0.241005	0.256157	0.712059
4	0.651316	0.709359	0.248608
5	0.228433	0.743842	0.460853
6	0.388549	0.522167	0.055658
7	0.950397	0.679802	0.523562
8	0.399487	0.344827	0.701298
9	0.109053	0.413793	0.670871
10	0.521988	0	0.670871
11	0.890938	0.522167	0
12	0.317565	0.497536	0.158441
13	0.571795	0.527093	0.642300
14	0.245094	0.034482	0.151391
15	0.484816	1	0.579591
16	0.788176	0.477832	0.292393
17	0.536575	0.778325	0.659369
18	0.331608	0.270935	0.061224
19	0.206959	0.330049	0.502040
20	0.818393	0.635467	0.352504
21	0.301674	0.241379	0.482003
22	0.586578	0.389162	0.377736
23	0.342361	0.556650	0.638218
24	0.578437	0.413793	0.309090
25	0.126369	0.408866	0.521706
26	1	0.532019	0.397031
27	0.339993	0.522167	0.585528
28	0.373212	0.576354	0.350278
29	0.394370	0.586206	0.481261
30	0.463568	0.546798	0.668645
31	0.399033	0.428571	0.310946
32	0.372959	0.596059	0.570686

Normalized values and deviational sequences for machining force, surface roughness and WST are depicted in Tables 2 and 3. Eigen values and Eigen vectors are depicted in Tables 4 and 5 respectively.
The weighting values of individual responses are predicted from squares of corresponding eigenvectors and are depicted in Table 5. The GRC and GRG for the experimental runs are given away in Table 6.

Table 4. Eigen values and explained variation for Principal components

Principal component	Eigen value	Explained variations (%)
First	0.6218	21.39
Second	1.244	42.8
Third	1.0405	35.8

Table 5. The Eigenvectors for principal components and contribution

Responses	Eigen vectors			Contribution
	First principal component	Second principal component	Third principal component	
Machining force	0.6542	-0.7268	-0.2093	0.427978
Surface roughness	-0.6272	-0.676	0.3867	0.39338
WST	0.4226	0.1217	0.8981	0.178591

Table 6. GRC, GRG and rank of the Machining force, Surface roughness and WST

Exp. No	GRC			GRG	Rank
	Machining force	Surface roughness	WST		
1	0.51779	0.45011	0.33333	0.48414	23
2	1	0.61329	0.57450	0.81700	1
3	0.67475	0.66123	0.41252	0.66471	6
4	0.43428	0.41344	0.66790	0.42823	27
5	0.68640	0.40198	0.52037	0.55398	12
6	0.56271	0.48915	0.89983	0.53410	16
7	0.34473	0.42379	0.48849	0.38300	32
8	0.55587	0.59183	0.41621	0.57025	10
9	0.82094	0.54716	0.42703	0.69002	4
10	0.48924	1	0.42703	0.72173	3
11	0.35946	0.48915	1	0.42822	28
12	0.61157	0.50123	0.75936	0.56335	11
13	0.46650	0.48681	0.43771	0.47537	24
14	0.67105	0.93548	0.76758	0.79334	2
15	0.50770	0.33333	0.46313	0.42737	29
16	0.38814	0.51133	0.63099	0.44804	25
17	0.48235	0.39113	0.43126	0.43992	26
18	0.60124	0.64856	0.89090	0.62717	9
19	0.70725	0.60237	0.49898	0.65625	7
20	0.37924	0.44034	0.58650	0.41024	30
21	0.62369	0.67441	0.50916	0.64519	8
22	0.46016	0.56232	0.56964	0.50848	20
23	0.59356	0.47319	0.43928	0.53629	15
24	0.46363	0.54716	0.61797	0.50410	21
25	0.79825	0.55013	0.48937	0.68031	5
26	0.33333	0.48448	0.55739	0.40573	31
27	0.59524	0.48915	0.46060	0.54478	14
28	0.57259	0.46453	0.58804	0.52345	17
29	0.55905	0.46031	0.50954	0.51321	19
30	0.51890	0.47764	0.42784	0.49871	22
31	0.55615	0.53846	0.61656	0.54897	13
32	0.57276	0.45617	0.46699	0.51793	18

3.2 Response surface methodology (RSM)

The Response Surface Methodology (RSM) was adopted for modeling and analysis of process parameters. In the RSM, relationship between response and independent input variables can be expressed as in equation (9):

$$GRG = F(\nu, f, d, r, \alpha) \quad (9)$$

Second-order quadratic regression model is fitted for GRG and the coefficients are estimated for 95% confidence level and hence those terms having P value >0.05 are insignificant shown in Table 7.

The model is developed in coded values and is given in equation (10):

$$\begin{aligned} GRG = {} & 0.095310\times\nu - 0.137378\times f - 0.073782\times d + \\ & 0.003972\times r - 0.143862\times\alpha + 0.063848\times d\times d \\ & - 0.139025\times\nu\times f + 0.060698\times\nu\times d \\ & - 0.117603\times f\times r + 0.060433\times\nu\times r \\ & + 0.093941\times r\times\alpha + 0.521633 \end{aligned} \quad (10)$$

Where ν Speed, f feed, d depth of cut, r nose radius, and α Negative rake angle.

R^2 value of 98.7% indicates that the model is in good agreement. The efficacy of the developed model is judged by the R^2 value and its value beyond 0.75 indicates the model is in good agreement [32].

Table 7. Estimated Regression Coefficients for GRG

Term	Coef	SE Coef	T	P	Importance
Constant	0.521633	0.008501	61.363	0.000	Significant
ν	0.095310	0.008701	10.954	0.000	Significant
f	-0.137378	0.008701	-15.789	0.000	Significant
d	-0.073782	0.008701	-8.480	0.000	Significant
r	0.003972	0.008701	0.456	0.006	Significant
α	-0.143862	0.008701	-16.534	0.000	Significant
ν·ν	0.020560	0.015740	1.306	0.218	Insignificant
f·f	0.020264	0.015740	1.287	0.224	Insignificant
d·d	0.063848	0.015740	4.056	0.002	Significant
r·r	0.007208	0.015740	0.458	0.656	Insignificant
α·α	0.030034	0.015740	1.908	0.083	Insignificant
ν·f	-0.139025	0.021313	-6.523	0.000	Significant
ν·d	0.060698	0.021313	2.848	0.016	Significant
ν·r	0.060433	0.021313	2.836	0.016	Significant
ν·α	-0.011620	0.021313	-0.545	0.597	Insignificant
f·d	0.025064	0.021313	1.176	0.264	Insignificant
f·r	-0.117603	0.021313	-5.518	0.000	Significant
f·α	0.025202	0.021313	1.183	0.262	Insignificant
d·r	0.023384	0.021313	1.097	0.296	Insignificant
d·α	0.042082	0.021313	1.974	0.074	Insignificant
r·α	0.093941	0.021313	4.408	0.001	Significant

S = 0.02131 R-Sq = 98.7% R-Sq(adj) = 96.4%

3.3 ANOVA analysis

ANOVA technique was used to test the adequacy of the developed response model. ANOVA test results were presented in Table 8, represents the adequacy of the model for 95% confidence level based on F ratio value.

Table 8. ANOVA for GRG

Source	DF	SS	MS	F	P	% Contribution
ν	4	0.0601	0.0150	1.22	0.325	16.63
f	4	0.1194	0.0299	2.96	0.038	33.05
d	4	0.0423	0.0106	0.82	0.526	11.71
r	4	0.0074	0.0018	0.13	0.970	2.04
α	4	0.13002	0.03251	3.35	0.024	35.99
Error	11	0.0018	0.0004			0.4983
Total	31	0.36102				

4. RESULTS AND DISCUSSION

In the present study, experiments were conducted as per the CCD of RSM. Multiple responses were condensed into a single entity called GRG using GRA and PCA. Modeling and optimization for GRG which is the indicating response for the three experimental results. Parametric influences and their interaction effects were discussed with main effects plot and response surface plots.

A better multiple-performance characteristic was obtained at the larger GRG. From the main effect plot (Figure 2), it is observed that the optimistic GRG acquired with Speed=1000rpm, feed=0.02mm/rev, depth of cut=0.4mm, nose radius=1mm and negative rake angle=5^o respectively.

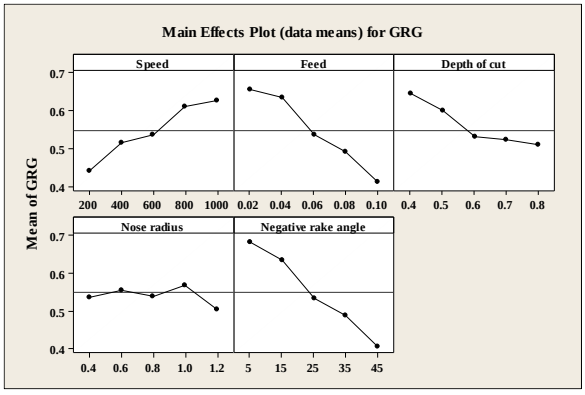

Fig. 2. Main effects plot

Table 9 shows the mean response table for GRG. In the response table (Table 9) it can be seen that negative rake angle has been assigned a rank 1 which means it is the most substantial parameter in controlling the response followed by feed, speed, depth of cut and nose radius. ANOVA used to estimate the percentage contribution of each machining parameters on multi-objective

optimization. From the ANOVA analysis, it is clear that negative rake angle has highest contribution (35.99%) succeeded by feed (33.05%) speed (16.63%) depth of cut (11.71%), nose radius (2.04%), and as depicted in Table 8.

Table 9. Mean response table for GRG

Level	Speed	Feed	Depth of cut	Nose Radius	Negative rake angle
1	0.4399	0.6563*	0.6452*	0.5363	0.6803*
2	0.5134	0.6337	0.5997	0.5544	0.6350
3	0.5412	0.5413	0.5316	0.5442	0.5391
4	0.6095	0.4892	0.5232	0.5684*	0.4879
5	0.6272*	0.4102	0.5085	0.5041	0.4057
Delta	0.1872	0.2460	0.1367	0.0643	0.2746
Rank	3	2	4	5	1

GRG for the acquired optimum of parametric combination was 0.984432 estimated from equation (11) and was 20.49% higher than highest GRG in Table 6.

$$\gamma = \gamma_m + \sum_{i=1}^{q} (\overline{\gamma_j} - \gamma_m) \qquad (11)$$

From the main effects plot (Figure 2) shows that grey relational grade increases significantly with an increase in speed which indexes the occurrence of optimum machining force, surface roughness and work piece surface temperature. It is attributed to the thermal softening of the material at the shear plane zone [33-35].

As feed increases grey relational grade reduces due to increase in cutting force which is attributed to more tool-chip interface and generation of helicoids furrows [36, 37]. Similar trend was observed with depth of cut due to the enhancement in cutting resistance & increase in maximum cutting edge angle [38, 39] apart from the aforesaid reasons.

Marginal variation in grey relational grade with an increase in nose radius is noticed. This is attributed to the variation in chip thickness & increased nose radius leads to reduction in surface roughness from general principles of metal cutting [40, 41].

Grey relational grade decreases significantly with an increase in negative rake angle. This is due to the increased edge strength of the tool with increase in negative rake angle causing ease in machining [38, 42]

The interaction among the parameters is discussed through the response surface plots shown in Figure 3 The higher GRG is noticed at the combinations of upper limits of speed due to thermal softening [33-35], lower limits of feed due to minimum cutting resistance and feed marks [43], lower limits of negative rake angle because of more cutting edge strength and ploughing energy [38, 40-41] and lower limits of depth of cut. However, the interaction of nose radius with other parameters is observed to be significant due to variation in chip thickness [41].

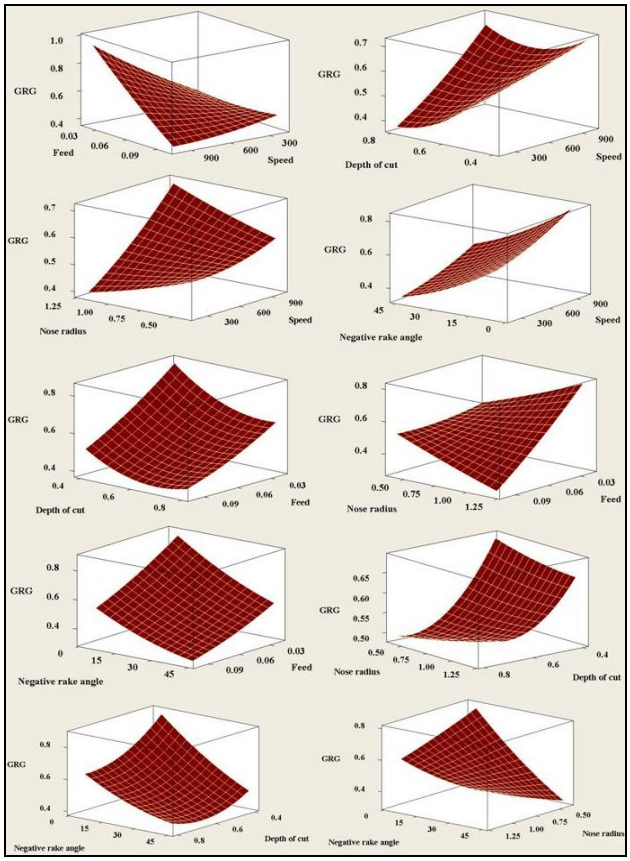

Fig. 3. Response surface plots [Hold values were Speed 600 rpm, Feed 0.06, Depth of cut 0.6, Nose radius 0.8, Negative rake angle 25]

5. CONFIRMATION TEST

The confirmation experiments were conducted by setting the process parameters at obtained optimum levels i.e cutting speed 800rpm, feed 0.04mm/rev, depth of cut 0.5mm, nose radius 0.6mm and negative rake angle 15°. The confirmation test results show considerable improvement in the machining performance and are given in Table 10.

Table 10. Grey relation grade values of initial, predicted, and confirmation

Setting level/ Responses		Optimal machining parameter A5B1C1D4E1	
	Initial data Expt. Run 2	Prediction	Experiment
Machining force	233.475		215.32
Surface roughness	0.465		0.418
WST	74.4		76.5
GRG	0.817007	0.984432	0.9233

6. CONCLUSIONS

The optimization of hard turning parameters with multiple responses (Machining force, surface roughness and WST) through AISI 52100 steel hard turning was carried out The experiments were conducted as per Center Composite Rotatable Design (CCD) of RSM and multi-objective optimization was performed adopting GRA integrated PCA.

The subsequent conclusions from this study are as follows.

•Multi-objective optimization index GRG increases significantly with increase in speed and decreases with feed, negative rake angle and depth of cut. Marginal variation is observed with nose radius.

•Optimum combination of the obtained parameters and their levels were A5B1C1D4E1 i.e (Speed=1000rpm, feed=0.02 mm/rev, depth of cut=0.4 mm, nose radius = 1 mm and negative rake angle = 5^o).

•Negative rake angle was observed to be the most sensitizing factor for multi object index followed by feed, speed, depth of cut and nose radius.

•The peak GRG is noticed at higher limits of speed, lower limits of feed, depth of cut, negative rake angle during interaction with other parameters.

•Mathematically predicted GRG and estimated GRG with confirmation experiment shows the improvement in the performance of hard turning which proves the adequacy of the adopted methodology.

•The surface roughness achieved is 0.418 microns which represents the soundness of dimensional accuracy and eliminates the necessity of further finishing process.

7. ACKNOWLEDGEMENT

Authors are grateful to Karunya Institute of Technology and Sciences, Coimbatore for providing facilities.

8. NOMENCLATURE AND ABBREVIATIONS

RSM - Response Surface Method
GRG- Grey Relation Grade
GRA- Grey Relation Analysis
GRC- Grey Relation Coefficient
PCA- Principle Component Analysis
ANOVA- Analysis of Variance
CBN- cubic boron nitride
PCBN- Polycrystalline cubic boron nitride
AISI- American Iron and Steel Institute
HRC - Hardness on Rockwell 'C' Scale
DOE- Design of Experiments
ν - Speed
f - Feed
d- Depth of cut
r- Nose radius
α- Negative rake angle
λ - Cutting edge Inclination angle
γ - Rake angle
α - Clearance angle
χ_r - Cutting edge angle
γ - Predicted Grey relational grade
γ_m - Total mean of Grey relational grade
$\overline{\gamma_j}$ - Mean of Grey relational grade at the optimal level
$x_i^0(k)$ - Measurement of the quality characteristic
$\max x_i^0(k)$ - largest value of $x_i^0(k)$
$\min x_i^0(k)$ - smallest value of $x_i^0(k)$

9. REFERENCES

1. König, W., Hochschule, T., Komanduri, R., Schenectady, D., Tönshoff, H.K., (1984). *Machining of hard materials*, CIRP Annals, **33**(2), 417–427.

2. König, W., Neises, A., (1993). *Wear mechanisms of ultrahard, nonmetallic cutting materials,* Wear, **162–164**, 12–21.

3. Tönshoff, H.K., Arendt, C., Amor, R.B., (2000). *Cutting of hardened steel*, CIRP Annals, **49**(2), 547–566.

4. Huang, O.Y., Chou, Y.K., Liang, Y.S., (2007). *CBN tool wear in hard turning: a survey on research progresses*, International Journal *of* Advanced Manufacturing Technology, **35**, 443-453.

5. Qinghua Li , Chen Pan, Yuxin Jiao and Kaixing Hu., (2018). *Research on PCBN Tool Dry Cutting GCr15*, Machines, **6**(28), 1-9.

6. Umamaheswarrao, P., Ranga Raju, D., NS Suman, K., Ravi Sankar, B., (2019). *Hybrid optimal scheme for minimizing machining force and surface roughness in hard turning of AISI 52100 steel*, International Journal of Engineering, Science and Technology, **11**(3), 19-29.

7. Avinash, K.L., Umamaheswarrao, P., Ravi Sankar, B., (2018). *Optimization of cutting force and Surface Roughness during hard turning of AISI 52100 steel*

using Hybrid GRA-PCA, Proceedings of 3rd International Conference on Advanced Manufacturing & Automation (INCAMA-2018), Krishnankoil, 1-10.
8. Amlana, P., Ashok Kumar, S., Arun Kumar, R., (2016). *Investigations on surface quality characteristics with multi-response parametric optimization and correlations,* Alexandria Engineering Journal, **55**, 1625–1633.
9. Dong Min, K., Do Young, K., and Hyung Wook, P., (2017). *Optimization of the Hard Turning Process of the Harden Bearing Steel Using Response Surface Methodology,* Journal of the Korean Society for Precision Engineering, **34**(10), 683-687.
10. Umamaheswarrao, P., Ranga Raju, D., NS Suman, K., Ravi Sankar, B., (2018). *Multi objective optimization of Process parameters for hard turning of AISI 52100 steel using Hybrid GRA-PCA,* Procedia Computer Science, **133**, 703–710.
11. Khamel, S., Ouelaa, N., Bouacha, K., (2012). *Analysis and prediction of tool wear, surface roughness and cutting forces in hard turning with CBN tool,* Journal of Mechanical Science and Technology, **26**(11), 3605-3616.
12. Bouacha, K., Yallese, M.A., Mabrouki, T., Rigal, J.F., (2010). *Statistical analysis of surface roughness and cutting forces using response surface methodology in hard turning of AISI 52100 bearing steel with CBN tool,* International Journal of Refractory Metals and Hard Materials, **28**, 349–361.
13. Das, S.R., Kumar, A., Debabrata, D., (2016). *Experimental investigation on cutting force and surface roughness in machining of hardened AISI 52100 steel using CBN tool,* International Journal of Machining and Machinability of Materials, **18**(5/6), 501–521.
14. Benga, G., Savu, D., Olei, A., (2015). *Influence of the cutting parameters on the Surface roughness when machining Hardened steel with ceramic and PCBN Cutting Tools,* Advanced Engineering Forum, **13**, 19-22, Trans Tech Publications Ltd, Switzerland.
15. Ravi Sankar, B., Umamaheswar rao, P., (2017). *Analysis of Forces during Hard Turning of AISI 52100 Steel Using Taguchi Method,* Materials Today Proceedings, **4**(2), pp. 2114–2118, Elsevier Ltd., Kidlington, UK.
16. Ravi Sankar, B., Umamaheswarrao, P., Nawaz Sharief, S.K., Suresh, T., Raju, R., (2017). *Parametric Investigations on Surface Roughness of Hard Turned AISI 52100 Steel,* Applied Mechanics and Materials, **867**, 171-176, Trans Tech Publications, Switzerland.
17. Suhail Adeel, H., Ismail, N., Wong, S.V., Abdul Jalil, N.A. (2010). *Optimization of Cutting Parameters Based on Surface Roughness and Assistance of Work piece Surface Temperature in Turning Process,* American Journal of Engineering and Applied Sciences, **3**(1), 102-108.
18. Suhail Adeel, H., Ismail, N., Wong, S.V., Abdul Jalil, N.A., (2012). *Surface roughness identification using the grey relational analysis with multiple performance characteristics in turning operations,* Arabian Journal for Science and Engineering, **37**(4), 1111–1117.
19. Das, S.R., Nayak, R.P., Dhupal, D., (2012). *optimization of cutting parameters on tool wear and workpiece surface temperature in turning of AISI D2 steel,* International Journal of Lean Thinking, **3**(2), 140-156.
20. Hardeep, S., Sumit, S., Vivek, A., Vineet, K., Sandeep, S., (2013). *Study of Cutting Parameters on Turning using EN9,* International Journal of Advance Industrial Engineering, **1**(2), 40-42.
21. Ravi Sankar, B., Umamaheswarrao, P., (2015). *Optimization of hardness and tensile strength of friction stir welded AA6061 alloy using response surface methodology coupled with grey relational analysis and principle component analysis,* International Journal of Engineering, Science and Technology, **7**(4), 21-29.
22. Pradhan, M.K., (2013). *Estimating the effect of process parameters on MRR, TWR and radial overcut of EDMed AISI D2 tool steel by RSM and GRA coupled with PCA,* International Journal *of* Advanced Manufacturing Technology, **68**(1-4), 591-605.
23. Vijayan, D., Rao, V.S., (2014). *Friction Stir Welding of Age-Hardenable Aluminum Alloys: A Parametric Approach Using RSM Based GRA Coupled With PCA,* Journal of The Institution of Engineers *(*India*):* Series C, **95**(2), 127–141.
24. Shailesh, D., Biswas, C.K., Soumya, G., (2014). *Optimization of the Surface Integrity Characteristics of EDM Process using PCA based Grey Relation Investigation,* Procedia Materials Science, **6**, 1091–1096.
25. Umamaheswarrao, P., Ranga Raju, D., NS Suman, K., Ravi Sankar, B., (2019). *Achieving optimal process parameters during Hard Turning of AISI 52100 Bearing Steel using Hybrid GRA-PCA,* Key Engineering Materials, **818**, 87-91, Trans Tech Publications Ltd, Switzerland.
26. Campos, P.H.S., Belinato, G., Paula, T.I., de Oliveira-Abans, M., Ferreira, J.R., Paiva, A.P., Balestrassi, P.P., (2017). *Multivariate mean square error for the multiobjective optimization of AISI 52100 hardened steel turning with wiper ceramic inserts tool: a comparative study,* Journal of the Brazilian Society of Mechanical Sciences and Engineering, **39**, 4021–4036.
27. Eskandari, B., Davoodi, B., Ghorbani, H., (2018). *Multi-objective optimization of parameters in turning of N-155 iron-nickel-base superalloy using gray*

relational analysis, Journal of the Brazilian Society of Mechanical Sciences and Engineering, **40**(4):233, DOI: 10.1007/s40430-018-1156-y.
28. Gupta, M., Kumar, S., (2013). *Multi-objective optimization of cutting parameters in turning using grey relational analysis*, International Journal of Industrial Engineering Computations, **4**, 547–558.
29. Wang, P., Meng, P., Zhai, J.Y., Zhou-Quan Zhu Z-Q. (2013). *A hybrid method using experiment design and grey relational analysis for multiple criteria decision making problems*, Knowledge-Based Systems, **53**, 100–107.
30. Pearson, K., (1901). *On lines and planes of closest fit RO systems of points in space*, Philosophical Magazine, **2**, 559-572.
31. Hotelling, H., (1993). *Analysis of a complex of statistical variables into principal components*, Journal of Educational Psychology, **24**, 417-441.
32. Le Man H, Behera S.K., Park H.S., (2010). *Optimization of operational parameters for ethanol production from Korean food waste leachate*, International Journal of Environmental Science and Technology, **7**(1), 157–164.
33. Ebrahimi, A., Moshksar, M.M., (2009). *Evaluation of machinability in turning of microalloyed and quenchedtempered steels: tool wear, statistical analysis, chip morphology*, Journal of materials processing technology, **209**, 910–921.
34. Lin, H.M., Liao, Y.S., Wei, C.C., (2008). *Wear behavior in turning high hardness alloy steel by CBN tool*, Wear, **264**, 679–684.
35. Yan, H., Hua, J., Shivpuri, R., (2005). *Numerical simulation of finish hard turning for AISI H13 die steel*, Science and Technology of Advanced Materials, **6**, 540–554.
36. Kumar, KVBSK, Choudhury, S.K., (2008). *Investigation of tool wear and cutting force in cryogenic machining using design of experiments*, Journal of materials processing technology, **203**, 95-101.
37. Aouici, H., Bouchelaghem, H., Yallese, M.A., Elbah, M., Fnides, B., (2014). *Machinability investigation in hard turning of AISI D3 cold work steel with ceramic tool using response surface methodology*, International Journal *of* Advanced Manufacturing Technology,**73**, 1775–1788.
38. Suresh, R., Basavarajappa, S., Gaitonde, V.N., Samuel, G.L., Paulo Davim, J., (2013). *State-of-the-art research in machinability of hardened steels*, Proceedings of the Institution of Mechanical Engineers Part B: Journal of Engineering Manufacturing, **227**(2), 191–209.
39. Sharma, V.S., Suresh Dhiman, Rakesh Sehgal, Sharma, S.K., (2008). *Estimation of cutting forces and surface roughness for hard turning using neural networks*, Journal of Intelligent Manufacturing, **19**(4), 473-483.
40. Chou, Y.K., Song, H., (2001). *Hard turning with different nose radius ceramic tools*, SME Technical Paper No. MR01-228,
41. Chou, Y.K., Song, H., (2004). *Tool nose radius effects on finish hard turning*, Journal of materials processing technology, **148**, 259–268.
42. Qian, L., Hossan, M.R. (2007). *Effect on cutting force in turning hardened tool steels with cubic boron nitride inserts*, Journal of materials processing technology, **191**(1–3), 274–278.
43. Azizi, M.W., Belhadi, S., Yallese, M.A., Lagred, A., Bouziane, A., Boulanouar, L., (2016). *Study of the machinability of Hardened 100Cr6 Bearing Steel with TiN coated Ceramic Inserts*. Proceedings of third International Conference on Energy, Materials, Applied Energetics and Pollution (ICEMAEP2016), Constantine, Algeria.

Received: June 14, 2019 / Accepted: December 15, 2019 / Paper available online: December 20, 2019 © International Journal of Modern Manufacturing Technologies